

Application of Dynamic Analysis and a Combination of Testing Methods in Modeling Soils Affected by a Strong Earthquake

Igwe Ogbonnaya

*Department of Geology, University of Nigeria, Nsukka, Enugu State
igwejames@hotmail.com*

and

Gratchev Ivan

*Department of Civil Engineering, University of Tokyo, Japan
ivangratchev@gmail.com*

ABSTRACT

A procedure is presented for modeling and investigating the pre and post-failure geotechnical characteristics of soils affected by strong earthquakes. Using a new method of dynamic numerical analysis and an experimental program aimed at understanding the post-failure behavior of such soils, it is shown that the resultant 0.74 factor of safety, 30 – 40 m failure elevation, critical failure plane and zero effective stress values are consistent with field work findings and observations. Compared to another method of stability analysis used in this research only the dynamic analysis provided the exact location of the most critical sliding surface. Laboratory undrained shear results on strongly weathered soils from the affected slopes show that after failure, generated excess pore water pressure was equal to the applied normal stress on the soils indicating that the soils liquefied and that they must have traveled down slope at considerable speed which correspond to the destruction and disruptions witnessed.

KEYWORDS: stability analysis, dynamic analysis, finite element method; zero effective stress, post-failure behavior.

INTRODUCTION

By its very nature, cyclic loading of slope soils present formidable challenges to geotechnical engineers regarding the most effective way to model the affected soils to reproduce vital aspects of the response of the soils. Representing the response of single (homogenous) elements of soil using some theoretical constitutive framework that is clear and concise is not simple. At each point during the formation of a constitutive model, problems of how best to regard the soil responses and the parameters defining those responses are challenging. As a reaction to these

challenges, so many models seeking same solution have resulted, with some being cumbersome or ineffective and others being just too simple to capture the whole truth. Dynamic analysis, as used in this paper, falls in between for its effectiveness and reliability of results.

SITE OF APPLICATION

The powerful Chuetsu Oki Earthquake with a magnitude 6.6 hit the northwest of Niigata Prefecture, Japan on July 17, 2007. The earthquake killed 11 people, injured about 2,000, caused the collapse of 1000 residential buildings and embankments, damaged important utilities including gas, electricity, water; and triggered massive landslides that blocked major railway lines. The Oumigawa landslide (Fig. 1) is just one such slope failures in the area of interest but have received a great deal of attention from the local government and the geotechnical community as it blocked the rail track near Oumigawa station JR, suspending train service for one month. A few days after the event, and in the days leading up to the present publication, survey of the sites of interest has been undertaken to evaluate the affected soils.



Figure 1: The site dynamic analysis was applied (The Oumigawa landslide, Niigata, Japan)

GENERAL PROCEDURE

The procedure used in this study include a series of triaxial tests on soil samples collected from the failure plane, slope stability analysis prior and after the earthquake, and dynamic analysis. On the basis of the obtained results, the mechanism of the Oumigawa landslide was clarified. It was also found that only the dynamic analysis provided the exact location of the most critical sliding surface, which was in a reasonably good agreement with the position of the sliding zone in the slope.

TESTS PROCEDURE

The dynamic properties of the soils were evaluated based on the results from a series of cyclic loading triaxial compression tests. After cyclic loading, static compression tests under undrained conditions were performed in order to obtain an indication of the strength remaining after the simulated earthquake loading. From the results of consolidated-drained triaxial compression tests, the strength parameters of the weathered soils on the slope of interest were found to be as follows: $\phi \approx 30^\circ$, and $c \approx 25$ kPa. The test data obtained from a series of undrained experiments produced the strength envelope that could be characterized by the parameter $\phi \approx 31^\circ$ and $c \approx 6$ kPa. It is noted that the difference between the strength parameters obtained from drained and undrained triaxial tests is very small, and can be seen only in a reduction of cohesion (c), probably due to the earthquake shaking. To understand the catastrophic behavior of soils that leave fatalities in the wake of an earthquake, the post-failure behavior of those soils would have to be scrutinized. In the light of this, an experimental program involving the use of a ring shear device which allows soils to be displaced for long distances was employed.

STABILITY ANALYSIS OF THE SLOPE BEFORE THE EARTHQUAKE

The stability of the slope before the earthquake was evaluated by means of the FEM computer code GUSLOPE developed at Gunma University, Japan. The strength parameters for the soil under consideration were established based on the test data from consolidated-drained triaxial compression tests. To simplify the analysis it was assumed that these soil characteristics were applicable down to the layer of volcanic conglomerate although in reality the soil was somewhat denser and stronger in the bottom. The stress-strain characteristics of other types of soil were established using published data for similar soils. Results of the slope stability analysis suggested that the slope was in a critical state prior to the earthquake as the safety factor calculated for the most critical failure plane was 1.02.

STABILITY ANALYSIS OF THE SLOPE AFTER THE EARTHQUAKE

To evaluate the stability of the slope after the earthquake, the strength parameters obtained from consolidated-undrained triaxial compression tests were used. Results of the slope stability analysis, which are presented in Fig. 2, indicated that the slope became unstable after the earthquake as the safety factor dropped to a value of 0.83. It is noted that the most critical failure plane had different shape and location than that observed immediately after the landslide during a rigorous fieldwork; that is, it was located deeper, and seemed to extend to the top of the slope. Thus, from the results presented in Fig. 2, it is inferred that the static analysis did not produce precise results with respect to the dynamics of the slide. For this reason, a different approach, which is referred to as dynamic analysis in this study, was used.

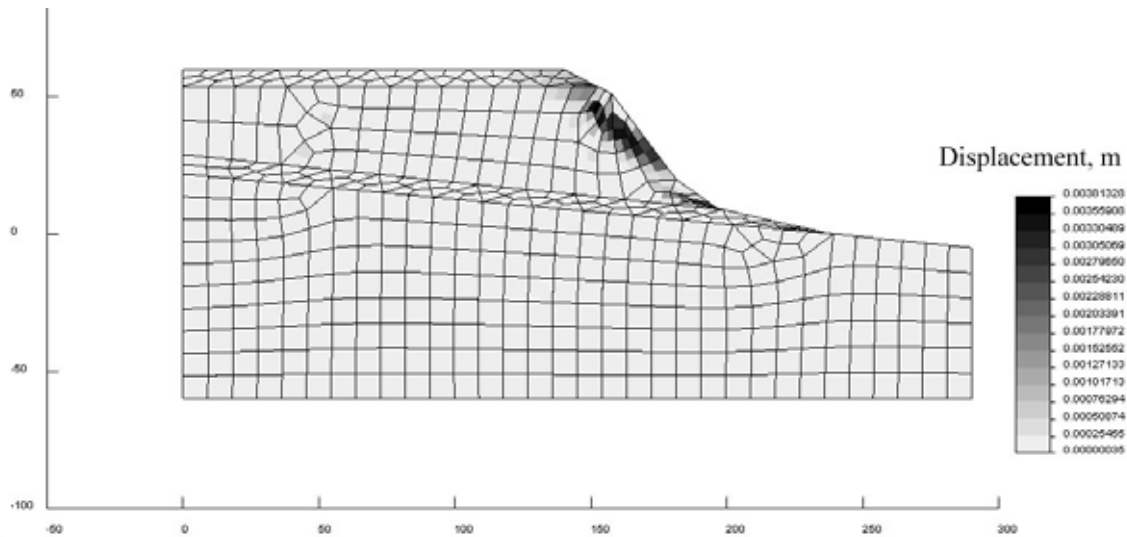


Figure 2: Stability analysis after earthquake conducted by FEM computer code GUSLOPE

DYNAMIC ANALYSIS: STEPS AND METHOD

The procedure used in this research was somewhat similar to that developed by Seed et al. (1969, 1975). It can be briefly described in the following 10 steps: (1) the initial stresses in the slope acting on the potential failure plane before the earthquake were determined; (2) the time history of shear stresses along the potential failure plane during the earthquake were determined, and represented by an equivalent number of regular load cycles (N); (3) the effects of the earthquake-induced stress on soil elements along the potential sliding surface were determined by conducting a series of cyclic triaxial tests on soil samples subjected to the combinations of pre-earthquake and superimposed dynamic stress conditions. (4) The peak shear stresses required to cause failure in N cycles at points along the potential sliding surface were determined and compared with the peak shear stresses induced by the earthquake on the same surface; (5) using the results obtained from cyclic tests, slope stability analysis was conducted to evaluate the safety factor of the slope after the earthquake. Details of this procedure are described in the following steps: (6) The initial stresses including overburden, lateral and shear stresses, along the failure plane of the weathered mass before the earthquake were evaluated by finite element computer code "2D Sigma".

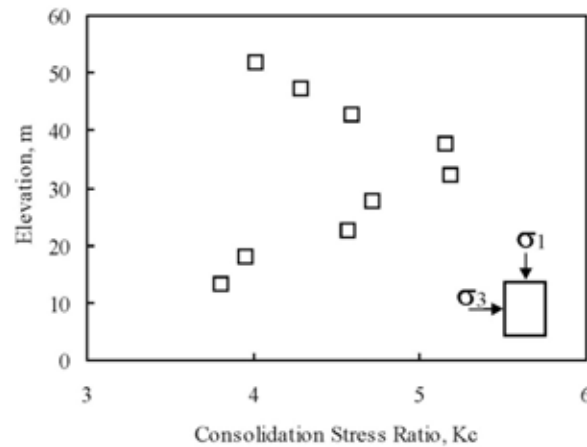


Figure 3: Distribution of consolidation stress ratio, $K_c = \sigma_1 / \sigma_3$, in the slope along the potential failure plane.

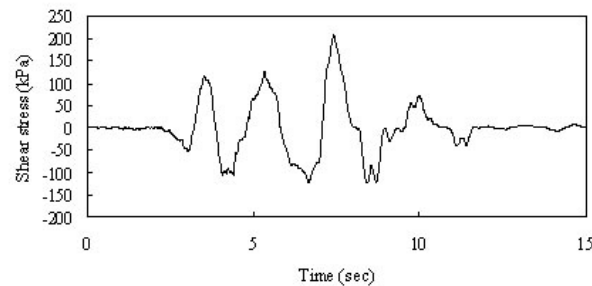


Figure 4: Time history of shear stresses at the site computed for the depth of 30 m.

These data were further utilized to calculate values of major and minor principal stress, σ_1 and σ_3 , parameters which were used in a series of triaxial tests to reproduce the initial stress conditions existing in the slope before the earthquake. In particular, it was found that a consolidation stress ratio, $K_c = \sigma_1 / \sigma_3$, (Fig. 3) varied in the slope from 4 to 5, reaching its maximum at the elevation of 30-40 m. (7) To evaluate the stresses acting on the failure plane during the Chuetsu Oki earthquake, the linear equivalent computer code “microShake” with strain-dependent modulus and damping was used. In this analysis, which is also known as “deconvolution” (Towhata, 2008), the ground motion record obtained at Kashiwazaki city by a K-net seismograph was first de-convolved to bed rock motion. Considering the distance between Kashiwazaki city and the landslide site, which was estimated to be about 10 km, the bed rock motion record was adjusted and then used to compute the time history of shear stresses at the Oumigawa landslide site. Finally, following up the procedure introduced by Seed et al. (1975), the time history of shear stresses was converted to an equivalent series of uniform cyclic stress applications (N). For example, it was found that the irregular earthquake loading at the elevation of 30 m (Fig. 4) could be represented by 5 regular load cycles with a cyclic stress ratio (CSR) of 0.42, $CSR = (0.65 * \tau_{max}) / \sigma$.

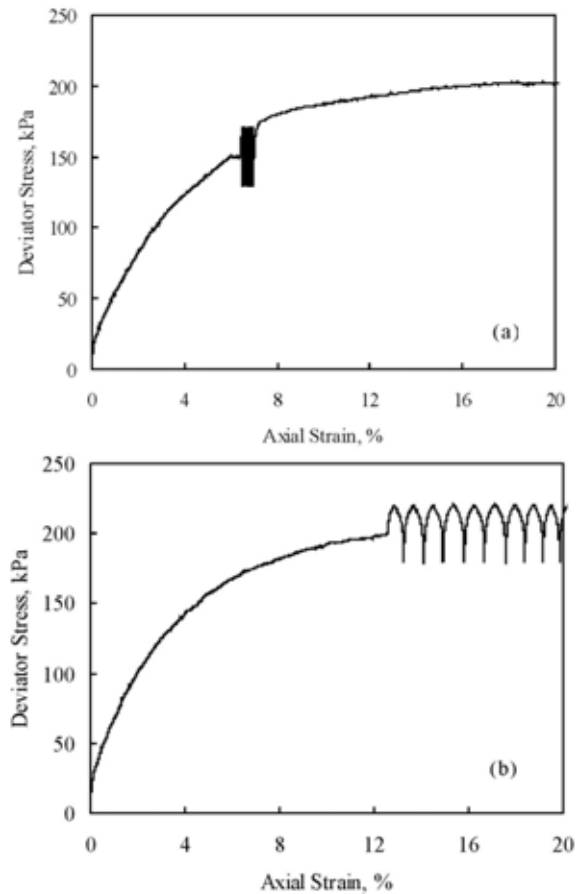


Figure 5: Results of cyclic loading undrained triaxial tests on anisotropically consolidated specimens: (a) $K_c=4.0$, $\sigma_3=50$ kPa; (b) $K_c=5.0$, $\sigma_3=50$ kPa.

(8) The dynamic properties of the mudstone were evaluated by conducting cyclic triaxial compression tests. The specimen prepared from slurry was consolidated to values of effective major and minor principal stresses, σ_1 and σ_3 that would cause the same normal shear stress on the potential failure plane as existed in a corresponding element in the slope. Values of σ_1 and σ_3 were obtained from the plots shown in Fig. 4. Following complete consolidation, the cyclic loading was applied under undrained conditions for 10 cycles or until the sample failed. After 10 cycles of loading, static compression tests under undrained conditions were performed in order to obtain an indication of the strength remaining after the simulated earthquake loading.

The results of two representative tests on specimens anisotropically consolidated to a consolidation stress ratios (K_c) of 4.0 (a), and 5.0 (b) with a confining pressure (σ_3) of 50 kPa are shown in Fig. 5. It is evident from this figure that in the case of $K_c=4.0$ (Fig. 5a), the soil retained some strength after the application of cyclic loading while, in the case of $K_c=5.0$ (Fig. 5b), the soil failed as the axial strain exceeded 15% after as few as 3 load cycles. (9) By using different values of the cyclic deviator stress (τ_d) and noting the number of cycles required to cause failure

(N), the cyclic deviator stresses required to cause failure in 5 cycles were determined for $K_c=4.0$, and 5.0. Summary of triaxial tests is presented in Fig. 6 in terms of cyclic stress ratio ($SCR=\tau_d/2\sigma_3$) against the number of cycles required to cause failure (N). From this plot it can be inferred that only for $K_c=5.0$, a parameter that corresponds to the stress conditions existing in the slope before the earthquake at the elevation of 30–40 m, the peak shear stresses induced by the earthquake ($CSR_{N=5}\approx 0.42$) exceeded the peak shear stresses ($CSR_{N=5}\approx 0.35$) required to cause failure in 5 cycles. This indicates that the earthquake may have triggered the failure at the elevation of 30-40 m.

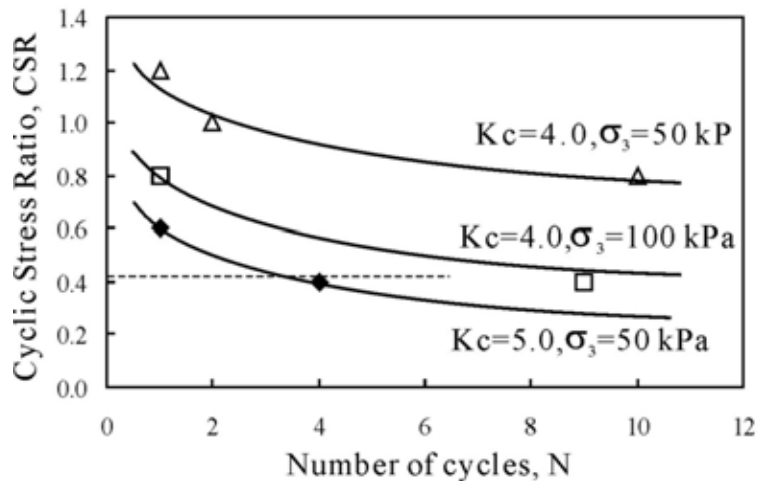


Figure 6: Results of cyclic loading undrained triaxial compression tests.

(10) Previous studies (Seed et al. 1969, 1975; Lee and Roth 1977) show that the governing parameters for an analysis of a slope after earthquakes are the static gravity driving stresses and the post-earthquake static strength of the soil after it was weakened by seismic shaking. The post-cyclic strength of the soil was obtained from the cyclic tests and post-cyclic undrained compression tests. Considering that the earthquake could have caused the failure of soil only at the elevation of 30-40 m, the post-earthquake stability of the slope was evaluated again by means of FEM procedure, yielding a smaller safety factor of 0.74. Moreover, the location of the most critical post-earthquake failure plane was in a reasonably good agreement with the position of the sliding zone in the slope (Fig. 7).

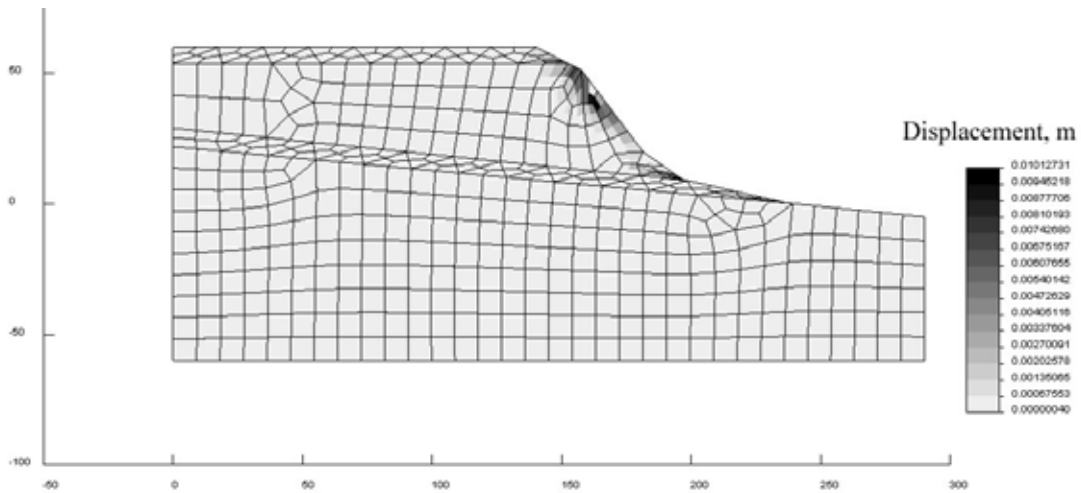


Figure 7: Results of slope stability analysis conducted by FEM computer code GUSLOPE using the dynamic approach.

POST-FAILURE MOBILITY OF AFFECTED SOILS

It's well-known that the behavior of soils under cyclic loading is controlled by effective stress or by the changes thereof, making knowledge of pore pressure generated during such loading a serious requirement for understanding the soils' behavior. Good models, be it numerical or physical, which are able to predict response of soils to static loading are also able, with adequate allowances and if necessary, modifications, to predict incremental responses of soils under cyclic loading. Post-failure behavior or mobility of soils affected by a powerful earthquake may therefore be assessed by static tests using a ring shear device that allows for unlimited shear displacement. The apparatus is structured to eliminate some difficulties commonly encountered with other more conventional apparatuses while studying the mechanism of landslide motion. It is equipped to allow speed-, and stress- controlled tests; and it's flexibility permits switch of test conditions, from drained to undrained, and vice versa, at any point in time during an experiment. Results of the post-failure mobility assessment show that generated excess pore water pressure is equal to normal stress, leaving the soils with zero effective stress values and high brittleness indexes. Fig. 8a shows the stress path of a strongly weathered soil from one of the sites consolidated to a void ratio of 0.92. Fig. 8b shows the relationship between stress, pore pressure and shear displacement.

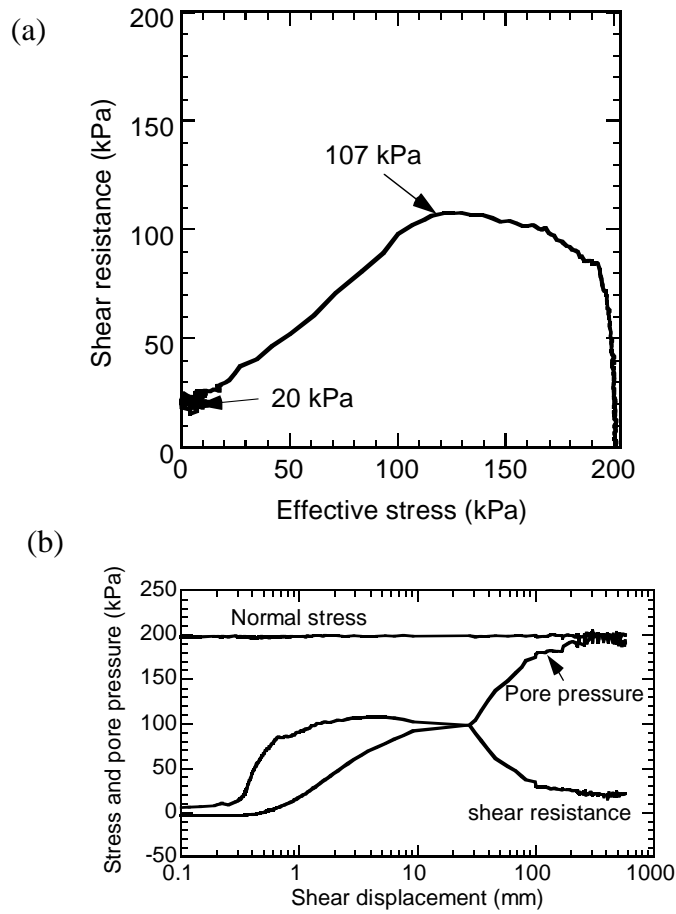


Figure 8: The undrained mechanical behavior of the strongly weathered soil

From the outset of shearing, pore pressure generation was evidently rapid and eventually reached the same value with the normal stress (200 kPa). Another specimen with a void ratio of 0.91 showed similar behavior of rapid and high excess pore water generation, Fig. 9a and b. Not only was the generation of pore pressure fast, it was also very high, reaching the value of normal stress.

The effective stress of the soil at steady state was almost zero which indicates the soil liquefied. This paper thinks that this may significantly explain the destructions and disruptions caused by the failure of the soils.

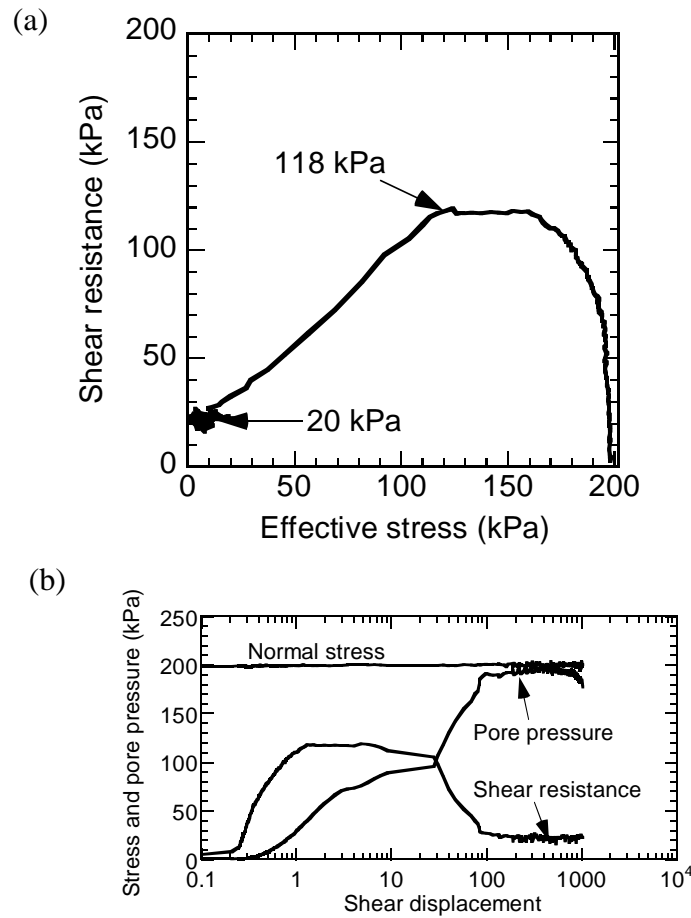


Figure 9: The undrained mechanical behavior of the strongly weathered soil

CONCLUSION

Results of laboratory tests combined with computer analysis of the stress conditions existing in the slope before, during and after the earthquake indicated that the slope appeared to be in a critical state before the earthquake. The earthquake generated seismic shear stresses that weakened the strength of the soil along the sliding surface. Although the decrease in the strength was not significant, it seemed to be sufficient to cause the slope instability. In addition, the cyclic test data indicated that the failure may have occurred at the elevation of 30-40 m. A finite element analysis (using the dynamic analysis method) conducted to evaluate the stability of the slope after the earthquake produced a small safety factor of 0.74, and the most critical failure plane, which was in a good agreement with the position of the sliding zone in the slope. Dynamic analysis provided results found more reliable than the static stability analysis method. Post-failure mobility investigation found that excess pore water pressure generated in the soils was equal to the normal stress on them. The soils therefore liquefied because their effective stresses at steady state are very low.

ACKNOWLEDGMENT

The authors would like to thank Mr. Akira Ezoe, a researcher from the University of Tokyo, for his significant help throughout this investigation. Valuable information concerning the geological conditions of the Oumigawa landslide was provided by Dr. Jorgen Johansson/Assistant Professor at the University of Tokyo. Special acknowledgement should be given to Professor Keizo Ugai and Assistant Professor Dr. Cai Fei from Gunma University for their kind permission to use computer code GUSLOPE for this research. The financial support was provided by The Japan Society for the Promotion of Science (JSPS).

REFERENCES

1. Lee, K., Roth, W. (1977) Seismic stability analysis of Hawkins Hydraulic fill dam.” Journal of the Geotechnical Engineering Division, ASCE, 103 (6), 627-644.
2. Seed, B., Lee, K., Idriss, I. (1969) Analysis of Sheffield dam failure.” Journal of the Soil Mechanics and Foundation Division, ASCE, 95 (6), 1453-1490.
3. Seed, B., Idriss, I., Lee, K. (1975) Dynamic analysis of the slide in the lower San Fernando dam during the earthquake of February 9, 1971. Sheffield dam failiure.” Journal of the Geotechnical Engineering Division, ASCE, 101 (9), 889-911.
4. Seed, B., Idriss, I., Makdisi, F., Banerjee, N. (1975) “Representation of irregular stress time histories by equivalent uniform stress series in liquefaction analyses.” Report N. EERC 75-29, California.
5. Towhata, I. (2008) Geotechnical Earthquake Engineering. Springer

